

# Theoretical and experimental analysis of the antioxidant features of diarylhydrazones

Swarada Peerannawar<sup>1</sup> · William Horton<sup>1</sup> · Anne Kokel<sup>1</sup> · Fanni Török<sup>1</sup> · Marianna Török<sup>1</sup> · Béla Török<sup>1</sup>

Received: 7 October 2016 / Accepted: 19 October 2016  
© Springer Science+Business Media New York 2016

**Abstract** Structural and energetic features of a series of 15 diarylhydrazone derivatives were studied via density functional theory (DFT) in order to identify the key features that most likely contribute to their antioxidant effect. Theoretical calculations were carried out at the B3LYP/6-31G(d,p) level. The calculated physicochemical parameters included the ionization potential, N-H dissociation enthalpy, proton affinity, HOMO/LUMO energies, and the band gaps of the most stable conformation of the compounds. To assess the contribution of these factors to the in vitro activity, the compounds were synthesized and their antioxidant activity was also determined in three commonly used assays. The hydrazones were evaluated for their radical scavenging against the 2,2-diphenyl-1-picrylhydrazyl (DPPH), 2,2'-azino-bis(3-ethylbenzthiazoline-6-sulphonic acid) (ABTS), and peroxy (ORAC assay) radicals. The experimental radical scavenging data of the compounds have been then plotted against the physicochemical characteristics and based on the obtained fits conclusions have been drawn regarding the relative importance of the respective factors.

**Keywords** Diarylhydrazones · Antioxidant capacity · Radical scavenging · DFT calculations · Structure-activity relationship

## Introduction

Oxidative stress is known to contribute to aging and the development and progression of various cancers and cardiovascular and neurodegenerative diseases [1]. The accumulation of excessive amounts of reactive oxygen and nitrogen species (ROS and RNS, respectively), often the result of environmental factors, intensify oxidative stress and thus may aggravate related disorders [2–4]. In addition to the body's biochemical defense mechanisms, dietary antioxidants are also important in shielding against the harmful effect of free radicals [5]. While some well-known exogenous natural product antioxidants contribute to cellular protection [1], poor pharmacokinetic properties often limit their therapeutic potential. Thus, extensive efforts have been made to improve the drug-like properties of natural antioxidants, through the chemical modification of their structures [5]. Several structure-activity relationship (SAR) and quantitative structure activity relationship (QSAR) studies were described in which the synthetic efforts were often coupled with biochemical, cell-based, and in silico screening methods to identify the most potent synthetic derivative of a natural antioxidant compound [6–10].

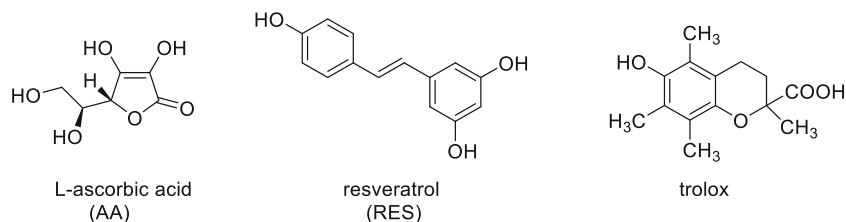
The stilbene derivative, resveratrol (Fig. 1a), is a common and potent dietary antioxidant; however, its ADME properties are insufficient [11]. The bridge between the aromatic rings is critical for its bioactivity [12] and increasing the bridge size improves the antioxidant activity [8]. Earlier, we have synthesized and applied several hydrazone derivatives as anti-Alzheimer's disease agents [13]. The compounds have a general structure (Scheme 1b), that makes their core a resveratrol mimic; however, the inclusion of the two nitrogen atoms improves the solubility, while other substituents may increase the membrane permeability. The molecules were found to be excellent inhibitors of the formation of neurotoxic amyloid  $\beta$  ( $A\beta$ ) self-assemblies and exhibited antioxidant properties as well [13].

✉ Marianna Török  
marianna.torok@umb.edu

✉ Béla Török  
bela.torok@umb.edu

<sup>1</sup> University of Massachusetts Boston, 100 Morrissey Blvd., Boston, MA, USA

**Fig. 1** Structure of three well-known, commercial antioxidants that were used as reference compounds in the present study



In this work, we continue to explore the antioxidant properties of the hydrazone derivatives, in order to identify key elements that contribute to the potency of the compounds. Density functional theory (DFT) methods are used to calculate several of their important physicochemical properties, and these data will be correlated to the experimental antioxidant activity determined in three radical scavenging assays.

## Experimental and theoretical methods

**General information—synthesis** The starting materials, the NMR reference compounds, were purchased from Aldrich. The NMR solvents (DMSO- $d_6$  and  $CDCl_3$ , 99.8 %) were Cambridge Isotope Laboratories products. Other solvents were purchased from Fisher. The mass spectrometric identification of the products was carried out by an Agilent 6850 gas chromatograph–5973 mass spectrometer system (70 eV electron impact ionization) (30 m long DB-5 column—J&W Scientific). The  $^1H$ ,  $^{13}C$ , and  $^{19}F$  NMR spectra were obtained on a 300-MHz Varian Gemini 300 and a 400-MHz Agilent

400MR NMR spectrometer, in DMSO- $d_6$  and  $CDCl_3$  with tetramethylsilane and  $CFCl_3$  as internal standards.

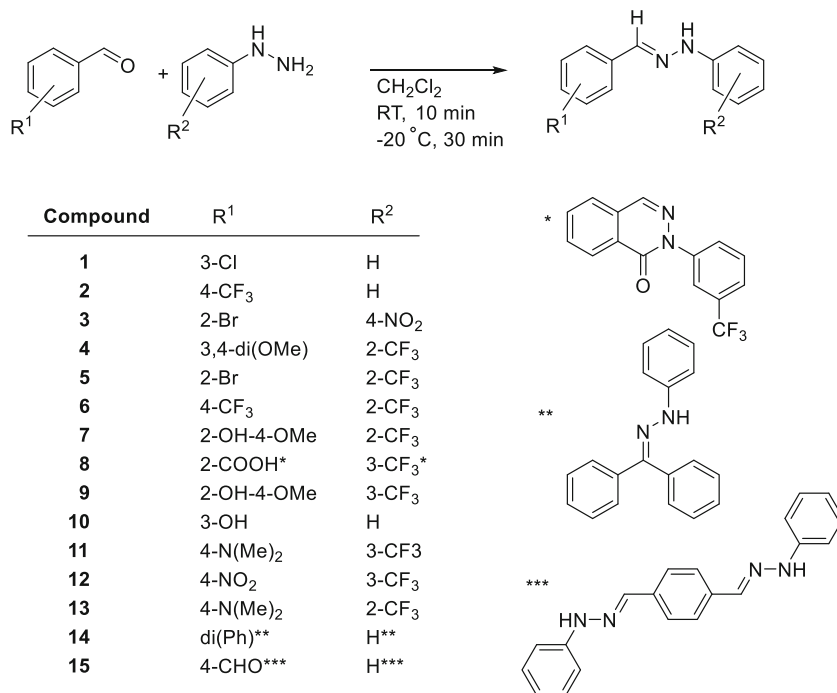
**General synthesis of the hydrazones** In a 25-mL Erlenmeyer flask, 1 mmol of benzaldehyde and 1 mmol of phenyl hydrazine were dissolved in 2 ml of dichloromethane. The reaction mixture was stirred for 10 min at room temperature, then it was cooled to  $-20^\circ C$  for 30 min to crystallize the product. The crystalline product was filtered and air-dried for 12 h. The purity was verified using GC-MS and NMR. Impurities were removed by recrystallization or preparative TLC to yield at least 98 % purity product.

Spectral data of the products:

### *(E)*-1-(3-chlorobenzylidene)-2-phenylhydrazine (**1**)

$^1H$  NMR (300.12 MHz,  $CDCl_3$ ),  $\delta$  (ppm) 7.66 (m, 4H), 7.29 (m, 2H), 7.13 (d, 2H,  $J = 6$  Hz), 6.93 (t, 1H, 6 Hz).  $^{13}C$  NMR (75.47 MHz,  $CDCl_3$ ), (ppm) 134.7, 139.8, 134.3, 132.4, 129.4, 126.2, 121.0, 119.1, 112.0, 110.91. MS:  $C_{13}H_{11}N_2Cl$  230 ( $M^+$ , 100 %); 92 (63 %); 229 ( $M^+ - 1$ , 31 %)

**Scheme 1** Synthesis and structures of the hydrazones studied



(E)-1-phenyl-2-(4-(trifluoromethyl)benzylidene)hydrazine (2)

$^1\text{H}$  NMR (300.12 MHz,  $\text{CDCl}_3$ ),  $\delta$  (ppm) 7.67 (d, 1H,  $J = 9$  Hz), 7.56 (m, 3H), 7.28 (t, 2H,  $J = 9$  Hz), 7.09 (d, 2H,  $J = 9$  Hz), 6.90 (t, 1H,  $J = 6$  Hz).  $^{13}\text{C}$  NMR (75.47 MHz,  $\text{CDCl}_3$ ), (ppm) 144.0, 135.1, 129.4, 126.1, 125.6, 125.5, 125.4, 120.7, 112.9.  $^{19}\text{F}$  NMR (300.12 MHz,  $\text{CDCl}_3$ ),  $\delta$  (ppm) -62.5. MS:  $\text{C}_{14}\text{H}_{11}\text{F}_3\text{N}_2$  264 ( $\text{M}^+$ , 100 %); 92 (58 %).

(E)-1-(2-bromobenzylidene)-2-(4-nitrophenyl)hydrazine (3)

$^1\text{H}$  NMR (300.12 MHz,  $\text{DMSO}-d_6$ ),  $\delta$  (ppm) 11.50 (br, 1H), 8.23 (s, 1H), 8.04 (d, 2H,  $J = 9$  Hz), 7.94 (d, 1H,  $J = 6$  Hz), 7.56 (d, 1H,  $J = 6$  Hz), 7.34 (t, 1H,  $J = 6$  Hz), 7.20 (t, 1H,  $J = 6$  Hz), 7.09 (d, 2H,  $J = 9$  Hz).  $^{13}\text{C}$  NMR (75.47 MHz,  $\text{DMSO}-d_6$ ), (ppm) 150.8, 140.3, 139.4, 133.9, 133.7, 131.4, 128.7, 127.4, 126.8, 123.2, 112.2. MS:  $\text{C}_{13}\text{H}_{10}\text{BrO}_2\text{N}_3$ : 91 (100 %); 207 (23 %)

(E)-1-(3,4-dimethoxybenzylidene)-2-(2-(trifluoromethyl)phenyl)hydrazine (4)

$^1\text{H}$  NMR (300.12 MHz,  $\text{CDCl}_3$ ),  $\delta$  (ppm) 7.94 (br, 1H), 7.77 (m, 2H), 7.48 (m, 2H), 7.38 (s, 1H), 7.08 (m, 1H), 6.88 (m, 1H), 3.97 (s, 3H), 3.92 (s, 3H).  $^{13}\text{C}$  NMR (75.47 MHz,  $\text{CDCl}_3$ ), (ppm) 150.2, 149.3, 140.3, 133.1, 127.7, 126.2, 126.1, 120.8, 118.7, 114.5, 110.7, 107.7, 55.9, 55.8.  $^{19}\text{F}$  NMR (300.12 MHz,  $\text{CDCl}_3$ ),  $\delta$  (ppm) -61.8. MS:  $\text{C}_{16}\text{H}_{15}\text{F}_3\text{O}_2\text{N}_2$ : 324 ( $\text{M}^+$ , 100 %); 138 (23 %).

(E)-1-(2-bromobenzylidene)-2-(2-(trifluoromethyl)phenyl)hydrazine (5)

$^1\text{H}$  NMR (300.12 MHz,  $\text{CDCl}_3$ ),  $\delta$  (ppm) 8.26 (br, 1H), 8.18 (s, 1H), 8.06 (d, 1H,  $J = 6$  Hz), 7.81 (d, 1H,  $J = 6$  Hz), 7.55 (m, 3H), 7.37 (m, 1H), 7.19 (t, 1H,  $J = 6$  Hz), 6.94 (t, 1H,  $J = 6$  Hz).  $^{13}\text{C}$  NMR (75.47 MHz,  $\text{CDCl}_3$ ), (ppm) 137.1, 138.6, 133.2, 133.1, 130.1, 127.5, 127.2, 126.2, 119.4, 114.8.  $^{19}\text{F}$  NMR (300.12 MHz,  $\text{CDCl}_3$ ),  $\delta$  (ppm) -60.9. MS:  $\text{C}_{14}\text{H}_9\text{F}_3\text{BrN}_2$ : 342 ( $\text{M}^+ - 1$ , 98 %); 243 (100 %).

(E)-1-(4-(trifluoromethyl)benzylidene)-2-(3-(trifluoromethyl)phenyl)hydrazine (6)

$^1\text{H}$  NMR (300.12 MHz,  $\text{CDCl}_3$ ),  $\delta$  (ppm) 8.17 (br, 1H), 7.80 (m, 4H), 7.63 (d, 2H,  $J = 6$  Hz), 7.50 (m, 2H), 6.95 (t, 1H,  $J = 6$  Hz).  $^{13}\text{C}$  NMR (75.47 MHz,  $\text{CDCl}_3$ ), (ppm) 138.4, 133.7, 126.9, 126.7, 126.7, 126.1, 126.0, 125.9, 120.1, 115.3.  $^{19}\text{F}$  NMR (300.12 MHz,  $\text{CDCl}_3$ ),  $\delta$  (ppm) -60.9, -62.7. MS:  $\text{C}_{15}\text{H}_{10}\text{F}_6\text{N}_2$ : 332 ( $\text{M}^+$ , 100 %); 160 (15 %).

(E)-5-methoxy-2-((2-(4-(trifluoromethyl)phenyl)hydrazono)methyl)phenol (7)

$^1\text{H}$  NMR (399.822 MHz,  $\text{DMSO}-d_6$ ),  $\delta$  (ppm): 10.51 (s, 1H), 8.10 (s, 1H), 7.49 (m, 2H), 7.15 (m, 2H), 7.01 (d, 1H), 6.46 (m, 2H), 3.85 (s, 3H). MS:  $\text{C}_{14}\text{H}_{13}\text{F}_3\text{O}_2\text{N}_2$ : 310 ( $\text{M}^+$ , 100 %); 161 (43 %)

2-(3-(trifluoromethyl)phenyl)phthalazin-1(2H)-one (8)

$^1\text{H}$  NMR (300.128 MHz,  $\text{CDCl}_3$ ),  $\delta$  (ppm): 8.53–8.50 (d, 1H,  $J = 7.5$  Hz), 8.32 (s, 1H, -CH), 8.02–7.76 (m, 5H), 7.64–7.61 (m, 2H);  $^{13}\text{C}$  NMR (75.466 MHz,  $\text{CDCl}_3$ ),  $\delta$  (ppm): 157.0, 139.0, 134.4, 133.8, 132.2, 130.8, 129.3, 129.1, 128.8, 128.3, 127.2, 126.3, 125.4, 124.2, 123.4, 122.6; MS  $\text{C}_{15}\text{H}_9\text{F}_3\text{N}_2\text{O}$ : 289 ( $\text{M}^+ - 1$ )

(E)-5-methoxy-2-((2-(3-(trifluoromethyl)phenyl)hydrazono)methyl)phenol (9)

$^1\text{H}$  NMR (300.128 MHz,  $\text{CDCl}_3$ ),  $\delta$  (ppm): 10.85 (s, 1H), 7.87 (s, 1H), 7.45–7.26 (m, 2H), 7.14–7.12 (m, 3H), 7.08–7.06 (d, 1H,  $J = 8.4$  Hz), 6.55 (s, 1H), 6.51–6.48 (d, 1H,  $J = 8.4$  Hz), 3.83 (s, 3H); MS  $\text{C}_{15}\text{H}_{13}\text{F}_3\text{N}_2\text{O}_2$ : 310 ( $\text{M}^+$ )

(E)-1-(3-hydroxybenzylidene)-2-phenylhydrazine (10)

$^1\text{H}$  NMR (399.822 MHz,  $\text{DMSO}-d_6$ ),  $\delta$  (ppm) 10.25 (s, 1H), 9.51 (br, s, 1H), 7.73 (s, 1H), 7.35–7.15 (m, 6H), 6.90–6.65 (m, 3H). MS:  $\text{C}_{13}\text{H}_{11}\text{N}_2\text{O}$  230 ( $\text{M}^+$ , 100 %); 92 (63 %); 229 ( $\text{M}^+ - 1$ , 31 %); MS:  $\text{C}_{13}\text{H}_{12}\text{ON}_2$ : 212 ( $\text{M}^+ - 1$ , 100 %); 92 (33 %)

(E)-N,N-dimethyl-4-((2-(3-(trifluoromethyl)phenyl)hydrazono)methyl)aniline (11)

$^1\text{H}$  NMR (300.128 MHz,  $\text{CDCl}_3$ ),  $\delta$  (ppm): 7.64 (s, 1H), 7.57–7.54 (m, 3H), 7.32–7.30 (m, 2H), 7.19–7.16 (d, 1H,  $J = 8.1$  Hz), 7.13 (m, 1H), 6.71 (m, 2H), 3.00 (s, 6H). MS:  $\text{C}_{16}\text{H}_{16}\text{F}_3\text{N}_3$ : 308 ( $\text{M}^+ + 1$ )

(E)-1-(4-nitrobenzylidene)-2-(3-(trifluoromethyl)phenyl)hydrazine (12)

$^1\text{H}$  NMR (300.12 MHz,  $\text{DMSO}-d_6$ ),  $\delta$  (ppm) 10.62 (br, 1H), 8.19 (d, 2H,  $J = 9$  Hz), 7.90 (s, 1H), 7.79 (d, 2H,  $J = 9$  Hz), 7.38 (m, 3H), 7.07 (d, 1H,  $J = 3$  Hz).  $^{13}\text{C}$  NMR (75.47 MHz,  $\text{DMSO}-d_6$ ), (ppm) 145.8, 144.2, 141.4, 134.1, 128.9, 125.3, 123.1, 115.3, 115.2, 115.1, 108.3, 108.2.  $^{19}\text{F}$  NMR (300.12 MHz,  $\text{DMSO}-d_6$ ),  $\delta$  (ppm) -62.5. MS:  $\text{C}_{14}\text{H}_{10}\text{F}_3\text{O}_2\text{N}_3$ : 309 ( $\text{M}^+$ , 100 %).

(E)-N,N-dimethyl-4-((2-(2-(trifluoromethyl)phenyl)hydrazono)methyl)aniline (13)

$^1\text{H}$  NMR (300.128 MHz,  $\text{CDCl}_3$ ),  $\delta$  (ppm): 7.80–7.74 (m, 2H, Ar -H, 1H, -CH), 7.58–7.55 (2H,  $J = 8.7$  Hz), 7.47–7.45 (m, 2H), 7.82 (m, 1H), 6.73–6.70 (d,  $J = 8.4$  Hz), 3.01 (s, 6H); MS  $\text{C}_{16}\text{H}_{16}\text{F}_3\text{N}_3$ : 307 ( $\text{M}^+$ )

1-(diphenylmethylene)-2-phenylhydrazine (14)

$^1\text{H}$  NMR (399.822 MHz,  $\text{DMSO}-d_6$ ),  $\delta$  (ppm): 8.75 (s, 1H), 7.61–7.57 (m, 2H), 7.41–7.25 (m, 5H), 7.22–7.08 (m, 7H), 6.72 (m, 1H); MS  $\text{C}_{20}\text{H}_{18}\text{N}_2$ : 272 ( $\text{M}^+$ , 100 %); 77 (30 %)

1,4-bis((E)-(2-phenylhydrazono)methyl)benzene (15)

$^1\text{H}$  NMR (399.822 MHz,  $\text{DMSO}-d_6$ ),  $\delta$  (ppm): 10.37 (s, 2H), 7.82 (s, 2H), 7.61 (s, 4H), 7.23–7.06 (m, 8H), 6.73 (m, 2H); MS  $\text{C}_{20}\text{H}_{18}\text{N}_4$ : 196 (100 %), 92 (37 %), 77 (15 %).

## Antioxidant assays

**ABTS assay [14]** The assay was carried out as described by Zou et al. [14] with minor modifications. Briefly, 0.015 g of 2,2'-azino-bis(3-ethylbenzthiazoline-6-sulphonic acid) (ABTS) and 0.002 g of  $K_2S_2O_8$  were dissolved in 4-mL water and diluted with 50 mM phosphate buffer (75 mM NaCl, pH = 7.4) until the observed absorbance at the wavelength of 734 nm was within 0.7–0.75. Stock solutions were prepared by dissolving trolox and resveratrol in ethanol (10 mM), ascorbic acid in water (10 mM), and diarylhydrazones in DMSO (50 mM), and then further diluted to 500  $\mu$ M with ethanol before use. The test compounds were assayed at 10  $\mu$ M final concentration. The absorbance values at a wavelength of 734 nm were recorded at 37 °C after 12 min using a VersaMax microplate reader equipped with SoftMax Pro 5 software (Molecular Devices). The reported percent radical scavenging activity (in percentile) was calculated using the  $[(A_c - A_t)/A_c] \times 100$  %, formula where  $A_c$  is absorption of the control that contained no antioxidant and  $A_t$  is the absorption obtained in the presence of the test/reference compounds.

**DPPH assay [13]** 2,2-diphenyl-picryl-hydrazyl (DPPH) stock solution was prepared in 50 % aqueous ethanol and the assay was carried out as described earlier [13]. Stock solutions at 10 mM concentrations were prepared by dissolving trolox and resveratrol in ethanol, ascorbic acid in water, and diarylhydrazones in DMSO then were further diluted to 200  $\mu$ M with ethanol before use. The final concentrations of DPPH and test compounds in the assays were 100 and 10  $\mu$ M, respectively. The absorbance values at a wavelength of 519 nm were recorded at 37 °C after 30 min using a VersaMax microplate reader equipped with SoftMax Pro 5 software (Molecular Devices). The reported percent radical scavenging activity was calculated by  $[(A_c - A_t)/A_c] \times 100$  %, where  $A_c$  is absorption of the control sample that contained no antioxidant and  $A_t$  is the absorption measured in the presence of the test/reference compounds.

**ORAC assay [15]** The ORAC assay followed the protocol developed by Huang et al. [15]. In short, fluorescein stock solution at the concentration of 4.19  $\mu$ M was prepared in 75 mM phosphate (pH = 7.4) buffer, freshly diluted with the same buffer to a concentration of 0.0816  $\mu$ M, and incubated at 37 °C for 15 min before the experiment. 2,2-azobis(2-amidinopropane) dihydrochloride (AAPH) was dissolved in the above buffer to a concentration of 153 mM. Stock solutions at 10 mM concentrations were prepared by dissolving trolox and resveratrol in ethanol, ascorbic acid in water, and diarylhydrazones in DMSO then were further diluted to 80  $\mu$ M with ethanol before use. The final concentrations of fluorescein and AAPH in the assays were 0.0612  $\mu$ M and 19.125 mM, respectively, while all test compounds were

assayed at 10  $\mu$ M final concentration. The maximum fluorescence intensity was recorded in every 2 min for a 60-min interval at 520-nm emission wavelength (with 485-nm excitation) at 37 °C using a SpectraMax i3 $\times$  microplate reader equipped with SoftMax Pro 6.5.1 (Molecular Devices) software. The reported percent radical scavenging activity was calculated by  $[(AUC_t - AUC_c)/AUC_{f\_max}] \times 100$  %, where  $AUC_t$  is the net area under the fluorescence curve obtained in the presence of the test/reference compounds,  $AUC_c$  is the net area under the fluorescence curve obtained for the control sample that contained no antioxidant (no test/reference compound), and  $AUC_{f\_max}$  is the net area under the fluorescence curve obtained for the maximum fluorescence control sample that contained no radical, thus had the maximum amount of fluorescein dye. The net area ( $AUC$ ) under the fluorescence curves was determined by the following equation:

$$\text{Net AUC} = 0.5 + \sum_{0-29} \frac{f_i}{f_0} + \left( 0.5 * \frac{f_{30}}{f_0} \right),$$

where  $f_0$  is the measured fluorescence intensity at time 0 and  $f_i$  is the measured fluorescence intensity at time  $i$ .

## Computational methods

Density functional theory has been employed to understand the electronic structure of hydrazones. All calculations were carried out at B3LYP/6-31G(d,p) [16] level of theory using Gaussian 09 program suite [17]. Frequency calculations for all compounds were performed to confirm the minima on potential energy surfaces. The effect of solvent (water) has also been studied for selected compounds to confirm their stability.  $^1\text{H}$  NMR chemical shifts ( $\delta\text{H}$ ) in DMSO for hydrazone and its azo tautomer were modeled by self-consistent reaction field (SCRF) calculations [18] by incorporating the polarizable continuum model (PCM). The chemical shifts were calculated by subtracting the nuclear magnetic shielding tensors of protons in the hydrazone and its tautomer from those of the tetramethylsilane (reference) using the gauge-independent atomic orbital (GIAO) method [19]. The N–H bond dissociation enthalpy (BDE) for all 15 compounds was obtained by subtracting the sum of enthalpy of the N-radical and hydrogen atom from that of the starting neutral compound. In addition to that, the N–H distance, dipole moment, logP value, ionization potential (IP), proton affinity (PA), the energy of the HOMO and LUMO orbitals, and the band gap were also calculated for all hydrazones to identify the possible correlation with experimental antioxidant activity.

## Results and discussion

Based on our earlier data, we have reported the 1,3-diarylhydrazone core structure as a potential lead for multifunctional therapeutic agents against Alzheimer's disease

(AD) [13]. As a part of the study, it was observed that the compounds showed substantial antioxidant effect. Such an effect is thought to be a significant part of the neuroprotective mechanisms against both the development and the progression of the disease [20]. In addition to AD, these properties could be beneficial in treating other disorders as well. Therefore, it is important to understand the impact of structural elements on the driving forces of antioxidant characteristics. Fifteen compounds have been selected and synthesized from the original group of hydrazones [13] and a few similar, novel structures have also been added. The compounds were subjected to three different antioxidant assays and structural analysis by density functional theory (DFT) methods. The syntheses of the compounds were carried out according to our previously described environmentally friendly method using a simple catalyst-free condensation of substituted benzaldehydes with aryl hydrazine derivatives (Scheme 1) [13]. The group of hydrazones included three related compounds that do not share the exact same core structure. The structures of these compounds (**8**, **14**, and **15**) are also shown in Scheme 1. Compounds **14** and **15** were synthesized using structurally different substrates (benzophenone and terephthalaldehyde, respectively) and in case of **8**, the starting material was 2-formyl-benzoic acid. However, after the condensation reaction that occurred between the formyl and  $\text{NH}_2$ -groups, the intermediate product underwent immediate cyclization when the  $\text{NH}$ -group of the hydrazone attacked the carbonyl carbon of the carboxylic acid in a nucleophilic reaction and the corresponding phthalazinone derivative was isolated.

Following synthesis, the compounds were subjected to three broadly accepted antioxidant assays such as the DPPH, [13] ABTS [14, 21], and ORAC [15, 22] assays. In order to put the observed effects into context, the activity of three well-known antioxidants, including ascorbic acid (AA) [23], resveratrol (RES) [13, 24], and trolox [25] (Fig. 1) were also assessed in the same assays. The data are shown in Fig. 2.

The data indicate that the antioxidants clearly interact with the radicals. They undergo reactions when they scavenge the radicals. Depending on the mechanism, different products can form (vide infra). The different activities observed in the assays were due to the (i) different radicals used and (ii) the different assay conditions. For this reason, it is customary to run several different assays to obtain a more general picture about the antioxidants. The error bars on Fig. 2 are well within 5–10 % indicating that the experiments for the individual assays were sufficiently reproducible.

The data reveal that the compounds showed a broad range of activity in the DPPH assay. Compound **8** exhibited no effect; several compounds appear to possess higher activities than those of the reference compounds (**7**, **9**, **15**) and the rest of the compounds showed moderate effect, similar to resveratrol; however, their radical scavenging effect is still higher than that of ascorbic acid and trolox. The data are somewhat similar in the ABTS assay; here, resveratrol is a very strong radical scavenger; however, according to the literature, this assay often reports false high radical scavenging for this compound due to several issues such as oxidation of the phenol or the generation of secondary products [26]. It was observed that only compound **10** is better than resveratrol, while the rest of the compounds showed varying effect (from 10 to 50 %) and most are yet more effective than ascorbic acid and trolox. The ORAC data diverges from the previous two sets. In this assay, the hydrazones appeared to be highly active, and although their radical scavenging is still somewhat lower than those of resveratrol and trolox, the activity values range from 50 to 88 % (except **8**, which remained inactive in the latter two assays as well). As a first observation, one can say that the compounds exhibit a strong structure-activity relationship in the DPPH and ABTS assays, while the studied limited variations of the substituents of the hydrazone core structure affect the antioxidant activity only in a moderate extent in the ORAC assay. It is important to note that compound **8**

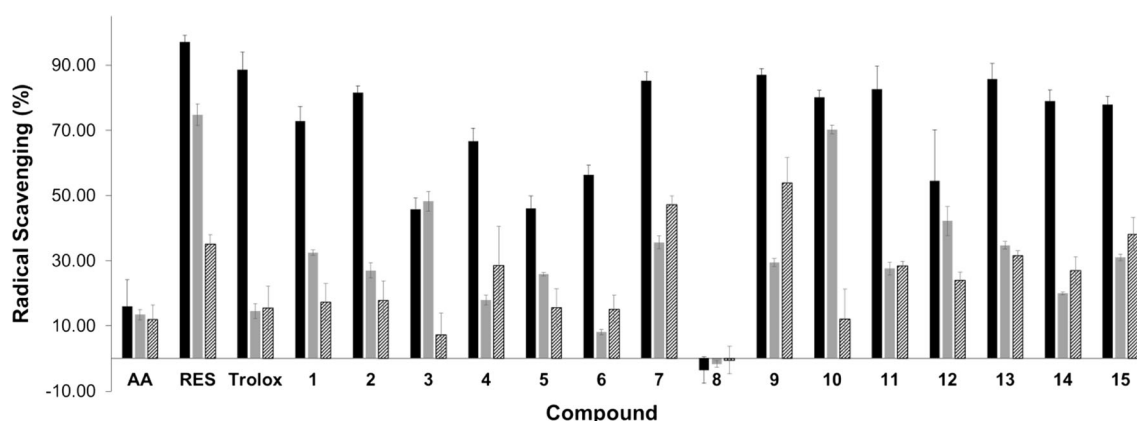


**Fig. 2** Antioxidant effect of the studied hydrazone derivatives (**1**–**15**) and three reference compounds (AA ascorbic acid, RES resveratrol, and Trolox) determined as their radical scavenging in the DPPH (pattern), ABTS (gray), and ORAC (black) assays at 10  $\mu\text{M}$  compound

concentration. Data are expressed as mean of % radical scavenging  $\pm$  standard deviation, where the number of independent repeats is 3



possessing a structure with no N–H bond uniformly did not exhibit any measurable effect.

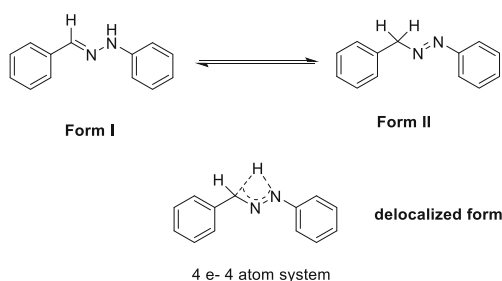
In regard to the contribution of the structural features, it is believed that the antioxidant activity of resveratrol is partially due to its phenolic OH groups as well as its conjugated structure. As the hydrazones possess a similar structure to RES, the possible contribution of the NH group as well as the partial conjugation was considered. The extended conjugation is a common characteristic in many natural antioxidants, such as lycopene (tomato),  $\beta$ -carotene (carrot), or curcumin (turmeric) [27]. It is proposed that the partial conjugation is achieved by the rapid equilibrium of the two potential tautomers of the hydrazones [28] as illustrated in Scheme 2.

First, the potential tautomeric forms of benzylidene-phenyl hydrazine (Scheme 2) have been investigated to reveal the stable form of the molecule, which would be the candidate for further calculations. The optimized geometry, electronic energy, and relative stabilization energy of the two tautomeric forms were calculated by Gaussian at the B3LYP/6-31G(d,p) level (Fig. 3).

The calculated relative stabilization energy data of the two resonance forms show that Form I with the  $\text{--C=N--NH--}$  unit is more stable than Form II with the  $\text{--CH}_2\text{--N=N--}$  unit by 9.9 kcal/mol. This energy difference between the tautomers is significant. Calculations revealed that the activation energy barrier between the Form I and Form II is  $E_A = 62.26$  kcal/mol, which is relatively high and supports the stabilization of hydrazone (Form\_I) over its azo tautomer (Form\_II). The structure of the transition state (Fig. 4a) and the intrinsic reaction coordinate diagram (Fig. 4b) are shown in Fig. 4.

Since the overall electron delocalization may also play a role in the antioxidant effect the electrostatic potential map of the tautomers has also been determined at isovalue 0.0004 (Fig. 5) in order to identify potential electron-rich or electron-deficient areas in the tautomers.

The electron density distribution appears to be significantly different in the case of the two tautomeric forms. Form I has more even electron distribution on the aromatic rings, and the vicinity of the N–H bond shows an electron-poor character. In contrast, Form II has an electron-rich area in the vicinity of the  $\text{N=N}$  bond due to the presence of the double bond as well as



**Scheme 2** Tautomers and the potential delocalized form of diarylhydrazones

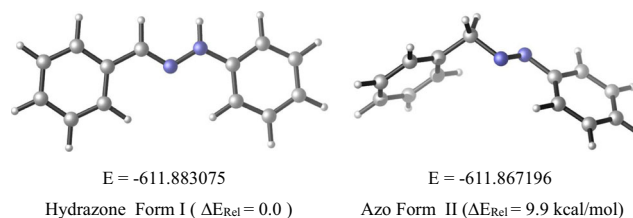


**Fig. 3** B3LYP/6-31G(d,p) optimized geometries of hydrazone Form\_I and azo Form\_II of benzylidene-phenyl hydrazine. Electronic energy ( $E$ ) is given in hartrees. Relative stabilization energies ( $\Delta E_{\text{rel}}$ ), expressed in kcal/mol, are given in parenthesis

the lone pairs of the N atoms. As a result, however, both aromatic rings exhibit a partially electron-poor character.

In order to investigate the tautomeric equilibrium both experimentally and theoretically, the  $^1\text{H}$  NMR spectrum of the benzylidene-phenyl hydrazine has been determined in  $\text{DMSO-}d_6$  and calculated for both tautomeric forms. The data are shown in Fig. 6.

The experimental spectrum is very similar to the calculated chemical shifts of the hydrazone form. The azo tautomer is only visible to a strongly limited extent; a small singlet appears at 5.750 ppm that represents the  $\text{CH}_2$  protons of the azo form. Therefore, the comparison of the theoretical and experimental  $^1\text{H}$  NMR data suggests that while the presence of the azo form is supported by the experimental spectrum, the contribution of this form appears to be negligible (less than 1 %). Thus, while the tautomeric equilibrium may contribute to a partially delocalized electron distribution, it likely is not a significant species in the radical scavenging processes that are related to the traditional mechanisms [29].

Based on the above studies, the hydrazone form was selected for further investigations in the case of the synthesized compounds. As these molecules (Scheme 1) contain a variety of substituents in altering positions, a conformational analysis was carried out to determine the lowest energy conformers that would be used to calculate the physicochemical parameters of the compounds for the structure-activity relationship studies. The optimized geometries and electronic energies of selected conformers are shown in Table 1.

The comparison of the electronic energies allowed the selection of the most stable conformers that were used to calculate the parameters of the compounds that we applied in the structure activity relationship studies. In several cases, the identification was a rather simple task, when the symmetry of the compound strongly favored a particular conformer. An interesting observation was made, however, when compounds with an OH substituent were investigated. The minimum energy structure of hydrazones 7 and 9 (Table 1, entries 7, 9, conformer 3) exposed an intramolecular hydrogen bonding interaction between the hydroxyl group and the  $\text{sp}^2$ -hybrid nitrogen from the hydrazone. As the phenolic OH group also participates in radical scavenging activity, this hydrogen bond

(a)

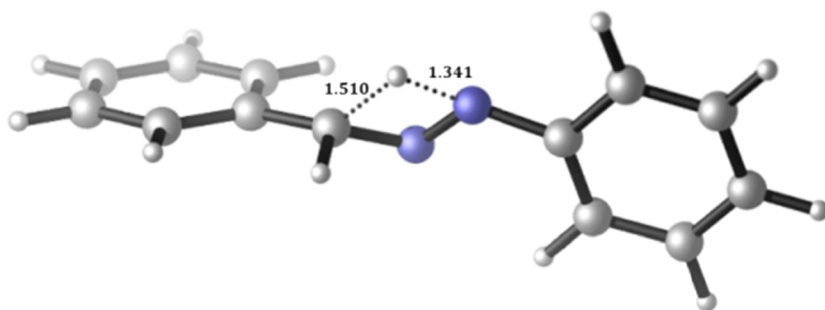
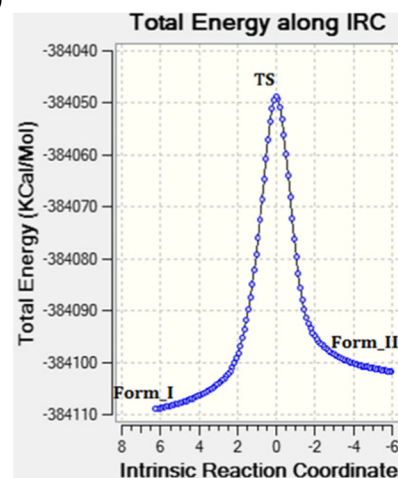


**Fig. 4 a** Transition state structure of the tautomeric process of benzylidene-phenyl hydrazine from hydrazone to azo form optimized at B3LYP/6-31G(d,p) level. Selected bond lengths are shown in angstrom. **b**

(b)



The intrinsic reaction coordinate vs. total energy diagram of the hydrazone to azo tautomeric transition

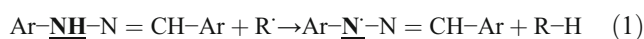
might affect its ability to perform that function. The calculations revealed a similar trend in conformational stability both in aqueous solution as well as in the gas phase indicating that the interaction with the water molecules does not disrupt the hydrogen bonding.

Finally, based on the data in Table 1, the lowest energy structures for each compound were selected for calculating the different parameters of the compounds to be used in the structure activity relationship studies. Several parameters such as N–H distance, dipole moment, logP value, HOMO–LUMO energies, band gap, bond dissociation enthalpy, proton affinity, and ionization potential were calculated. The data are tabulated in Table 2.

In order to uncover the potential contribution of the above-calculated parameters to the antioxidant activity, the relation of the parameters to the experimental data has been assessed. The activity of the compounds determined in the three assays was plotted versus each parameter. A few representative functions are shown in Fig. 7.

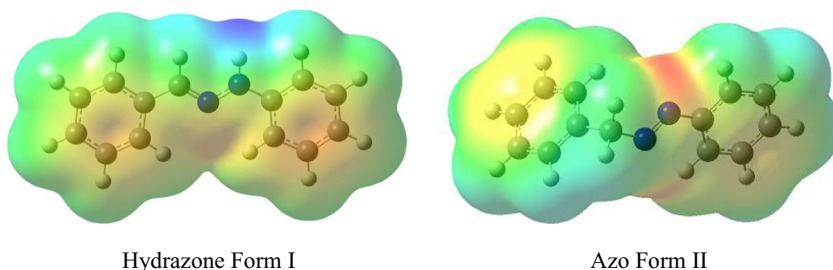
The analysis of the activity vs. property plots revealed that several parameters appear to influence the antioxidant activity while others seem to have no or only non-characteristic effects. Foremost, the N–H bond dissociation energies (BDE) showed a correlation with the antioxidant activity. Based on

the plots, obtained for the ORAC and DPPH assays (Fig. 7a, b, respectively), a parabolic relationship describes the effect of N–H BDE on the antioxidant activity, suggesting that from a central point, decreasing and increasing BDE values result in increasing activity. The BDE effect is a clear indication that the hydrazones, at least partially, act via the hydrogen atom transfer (HAT) mechanism as described in Eq. 1. The HAT mechanism is the most common mechanism considered for the natural antioxidant polyphenols [30]. However, the exponential correlation also indicates that while BDE is a strong contributing factor to the activity, it likely is not the only important characteristic.

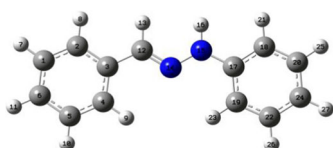
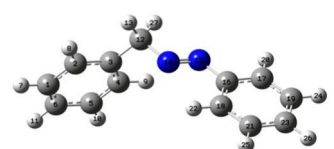


The underlying principle of the HAT mechanism is that low BDE indicates weak X–H bonds (X=N, O) which facilitate homolytic bond cleavage, thus providing H atoms to scavenge the target radical. Such a relationship is often observed for phenol derivatives, although the type of correlation varies [31]. It is important to note that compound 8, which does not possess an N–H bond, did not show any activity in either assay, a clear indication that the presence of the N–H bond is a necessary feature in these compounds. When comparing the calculated BDE with the

**Fig. 5** Electrostatic potential map shown for hydrazone Form I and azo Form II of benzylidene-phenyl hydrazine at isovalue 0.0004. The blue region shows electron-poor areas and the red region shows electron-rich surfaces



**Fig. 6** Calculated  $^1\text{H}$  NMR chemical shifts of the hydrazone form I and azo form II of benzylidene-phenyl hydrazine in DMSO

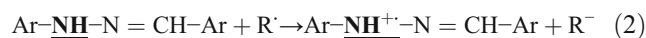
Hydrazone Form I		Azo Form II		Structures
H-atom number	$\delta_{\text{H-CALC}}$ (ppm)	H-atom number	$\delta_{\text{H-CALC}}$ (ppm)	
8	7.4	8	8.2	<i>Form I</i> 
7	7.6	7	7.8	
11	7.5	11	7.6	
10	7.6	10	7.6	
9	8.3	9	7.5	
21	6.8	22	7.8	
25	7.5	25	7.7	<i>Form II</i> 
27	7.0	26	7.8	
26	7.5	24	7.9	
23	7.6	20	8.3	
13	7.5	13	5.9	
16	7.9	17	4.9	

experimentally observed antioxidant activity, it was found that compounds **7**, **9**, **10**, and **13** show high experimental activities and have a low BDE; however, there are compounds, such as **11**, which have high BDE but also high activity in the assays. It must be noted that as the target radicals vary in the three assays, so does the correlation. Compounds **7**, **9**, and **10** represent a specific group in which the compounds also possess a phenolic OH group in addition to the NH group of the hydrazone linkage. Similarly, in three-ring, hydrazone-like compounds, the phenolic OH group was claimed to be primary antioxidant, despite obtaining lower BDE values for the NH bond than for the OH bond [32]. Thus, to evaluate the reactivity of the NH- and OH groups in these compounds, BDE of the OH bond was calculated. The obtained BDE values for the -O-H bonds are 77.5 (**7**), 77.1 (**9**), and 73.8 (**10**) kcal/mol. These values are comparatively higher than those calculated for the N-H bond in the same compounds: 64.75 (**7**), 64.02 (**9**), and 66.18 (**10**) kcal/mol. In addition, several compounds (e.g., **2**, **11**, **13**, **14**) that do not have phenolic OH substituent exhibit similar or better antioxidant activities than those with it. Thus, our data provide further support to the earlier observations regarding the relative N-H vs O-H BDE values; however, in contrast to the earlier suggestion [32], we found that the NH group is more efficient in the hydrogen atom transfer than the OH in these compounds.

It is worth noting that just like molecules **7**, **9** and **10**, compound **15** also contains multiple X-H bonds (two N-H) that may contribute positively to the antioxidant effect. The BDE of **15** (89.85 kcal/mol) is one of the highest in the studied groups despite that **15** exhibits one of the best activities. It is in line with the obtained exponential correlation; however, it also highlights that the number of active groups plays an important role.

Another important feature appears to be the ionization potential (IP). A representative plot is shown in Fig. 7c for the ORAC assay; however, similar correlation was observed in the other assays as well. The data indicate a linear relationship between IP and the antioxidant activity, namely, the activity

decreases with increasing IP. This finding suggests that the radical scavenging by hydrazones is partially due to their participation in the single electron transfer (SET) mechanism [33]. This pathway occurs in three steps as shown in Eqs. 2–4.

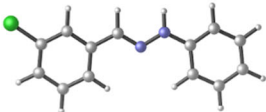
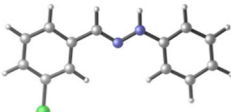
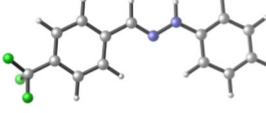
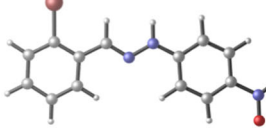
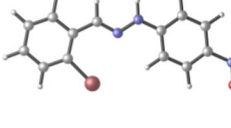
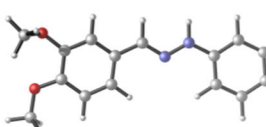
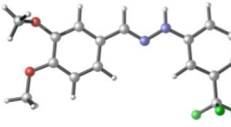
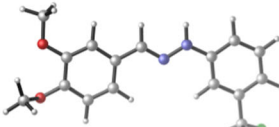
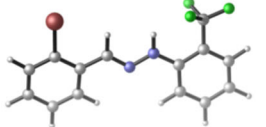
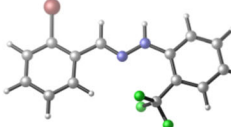
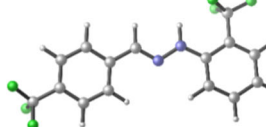
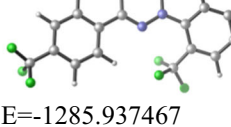
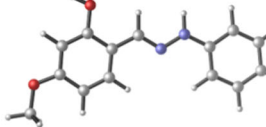
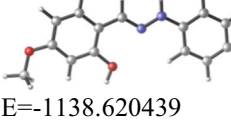
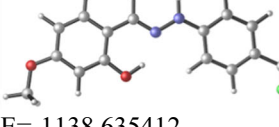
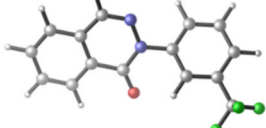
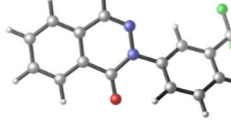


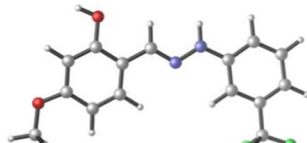
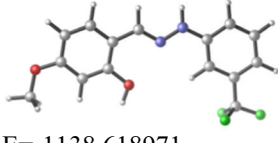
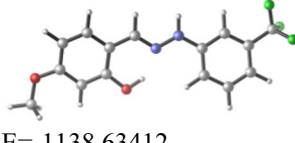
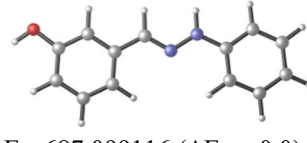
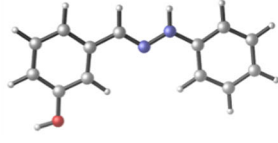
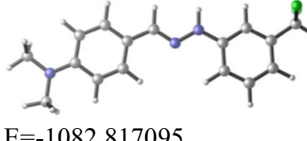
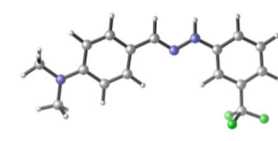
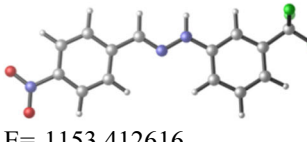
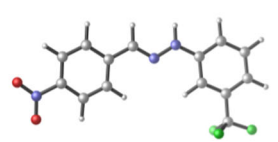
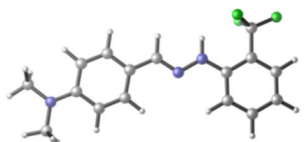
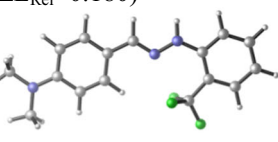
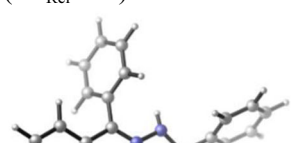
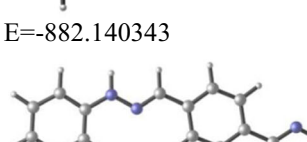
According to the data and Eq. 2, the increasing IP value will decrease the extent of the formation of the  $\text{Ar}-\underline{\text{NH}}^{\cdot+}-\text{N}=\text{CH}-\text{Ar}$  radical cation and thus result in diminishing antioxidant activity. Compounds with low IP values, such as **11**, **13**, **14**, and **15**, either having no additional substituents or the presence of electron withdrawing and electron donating substituents is balanced, appear to have high activities. In contrast, the exclusive presence of electron withdrawing groups on both rings of the hydrazones in **3** (Br,  $\text{NO}_2$ ), **5** (Br,  $\text{CF}_3$ ), **6** ( $\text{CF}_3$ ,  $\text{CF}_3$ ), and **12** ( $\text{NO}_2$ ,  $\text{CF}_3$ ) decreases the possibility of electron transfer from the parent compound, hence decreases the antioxidant activity.

In addition to the above-discussed molecular features, the logP value that describes the partition of the compounds in aqueous and organic media is a common factor to consider in structure-activity relationship studies. As an example, the effect of logP on the antioxidant activity is shown in Fig. 7d. The diagram indicates that increasing lipophilicity (or logP) results in decreasing antioxidant effect. This effect can be explained by the assay conditions; all assays are carried out in hydrophilic medium, either in aqueous buffers or 50 % aq. ethanol solution. Thus, compound **10** with a hydrophilic OH substituent showed the highest activity in the ABTS assay. However, when considering the logP factor, one must



**Table 1** B3LYP/6-31G(d,p) optimized geometries of hydrazone conformers

Compound	Conformer 1	Conformer 2	Conformer 3	Selected conformer
1	 E=-1071.487170 ( $\Delta E_{\text{Rel}}=0.005$ )	 E=-1071.487178 ( $\Delta E_{\text{Rel}}=0.0$ )		2
2	 E=-948.914773			1
3	 E=-3387.496664 ( $\Delta E_{\text{Rel}}=0.0$ )	 E=-3387.492026 ( $\Delta E_{\text{Rel}}=2.910$ )		1
4	 E=-1177.893122 ( $\Delta E_{\text{Rel}}=0.0$ )	 E=-1177.893017 ( $\Delta E_{\text{Rel}}=0.060$ )	 E=-1177.892232 ( $\Delta E_{\text{Rel}}=0.492$ )	1
5	 E=-3520.02675 ( $\Delta E_{\text{Rel}}=0.0$ )	 E=-3520.018558 ( $\Delta E_{\text{Rel}}=5.140$ )		1
6	 E=-1285.945827 ( $\Delta E_{\text{Rel}}=0.0$ )	 E=-1285.937467 ( $\Delta E_{\text{Rel}}=5.245$ )		1
7	 E=-1138.625669 ( $\Delta E_{\text{Rel}}=6.113$ )	 E=-1138.620439 ( $\Delta E_{\text{Rel}}=9.395$ )	 E=-1138.635412 ( $\Delta E_{\text{Rel}}=0.0$ )	3
8	 E=-1061.073094 ( $\Delta E_{\text{Rel}}=0.1$ )	 E=-1061.073402 ( $\Delta E_{\text{Rel}}=0.0$ )		2

9	 E=-1138.624073 ( $\Delta E_{\text{Rel}}$ =6.304)	 E=-1138.618971 ( $\Delta E_{\text{Rel}}$ =9.506)	 E=-1138.63412 ( $\Delta E_{\text{Rel}}$ =0.0)	3
10	 E=-687.099116 ( $\Delta E_{\text{Rel}}$ =0.0)	 E=-687.098919 ( $\Delta E_{\text{Rel}}$ =0.123)		1
11	 E=-1082.817095 ( $\Delta E_{\text{Rel}}$ =0.0)	 E=-1082.816944 ( $\Delta E_{\text{Rel}}$ =0.094)		1
12	 E=-1153.412616 ( $\Delta E_{\text{Rel}}$ =0.0)	 E=-1153.412329 ( $\Delta E_{\text{Rel}}$ =0.180)		1
13	 E=-1082.817245 ( $\Delta E_{\text{Rel}}$ =0.0)	 E=-1082.807854 ( $\Delta E_{\text{Rel}}$ =5.892)		1
14	 E=-882.140343			1
15	 E=-991.609857			1

Electronic energy (E) are given in hartree while the relative stabilization energies ( $\Delta E_{\text{Rel}}$ ) are in parenthesis in kcal/mol units.

remember that for compounds to be considered as drug candidates, they must also possess a reasonable lipophilicity as well.

The analysis of the other calculated physicochemical characteristics did not reveal significant correlation with the antioxidant activity.

The above results highlight clear and firm relationships between the structural and energetic features and their contribution to antioxidant activity for the studied group of hydrazones. However, it must be noted that an extended study with a broader group of hydrazones bearing more diverse substituents is needed to propose a

**Table 2** Calculated molecular descriptors for hydrazone derivatives

Compound	N–H distance (Å)	Dipole moment (Debye)	LogP <sub>o/w</sub>	HOMO (hartree)	LUMO (hartree)	Band gap (eV)	BDE (kcal/mol)	PA (kcal/mol)	IP	
									eV	kcal/mol
1	1.017	3.570	3.62	−0.19413	−0.05095	3.89	66.85	209.4	6.76	155.97
2	1.017	3.402	4.44	−0.19775	−0.05814	3.79	67.25	210.4	6.85	158.06
3	1.017	8.315	3.10	−0.2165	−0.08302	3.63	69.27	199.4	7.24	167.00
4	1.016	4.658	4.44	−0.18963	−0.04327	3.98	66.29	214.8	6.44	148.58
5	1.014	1.748	4.77	−0.20307	−0.05814	3.94	69.90	210.8	6.92	159.70
6	1.015	2.054	5.24	−0.20854	−0.06511	3.90	70.19	207.3	7.08	163.47
7	1.014	3.580	3.68	−0.19371	−0.04857	3.94	64.75	211.5	6.58	151.85
8	N/A	5.449	4.08	−0.22997	−0.06666	4.44	87.4	193.84	7.65	176.43
9	1.014	3.053	3.68	−0.19202	−0.04656	3.95	64.02	212.5	6.54	150.9
10	1.016	0.804	2.48	−0.18701	−0.04027	3.99	66.68	213.3	6.56	151.45
11	1.016	5.728	4.75	−0.17504	−0.03387	3.84	98.60	218.0	6.07	140.13
12	1.017	5.812	3.51	−0.21777	−0.09755	3.2	68.59	198.0	7.32	168.97
13	1.014	3.891	4.77	−0.17452	−0.033	3.85	67.86	221.05	6.05	139.55
14	1.020	2.276	5.51	−0.19515	−0.03277	4.41	92.02	232.6	6.44	148.59
15	1.017	0.197	4.37	−0.17781	−0.05797	3.26	89.86	218.0	5.99	138.16

Bond distance (in Å); dipole moment in Debye, logP<sub>o/w</sub>; HOMO and LUMO energies in hartrees; band gap in eV; bond dissociation enthalpy (BDE, in kcal/mol); proton affinity (PA, in kcal/mol); ionization potential (IP, in eV and kcal/mol)

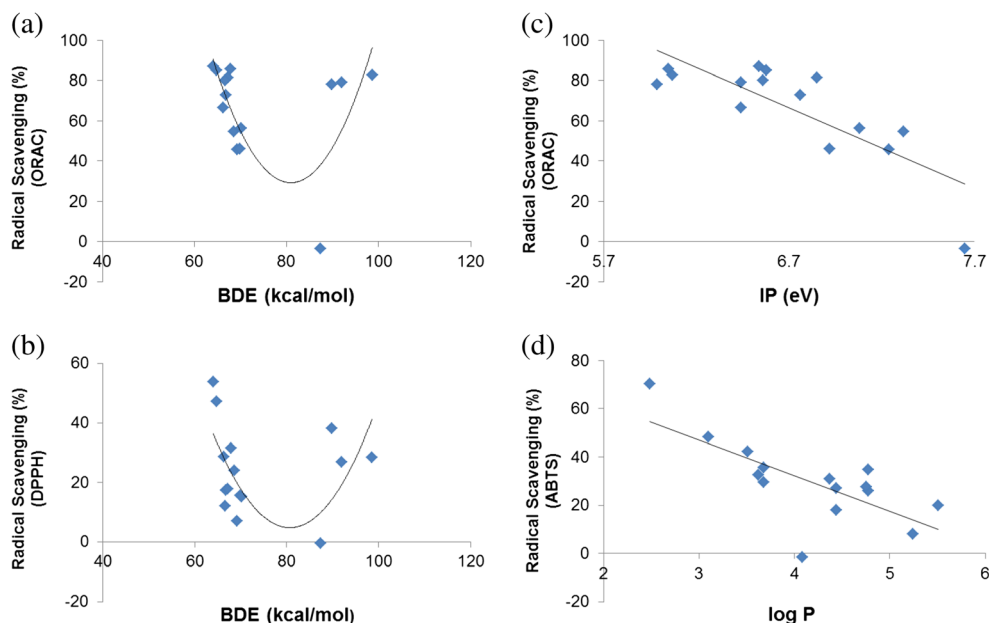
quantitative description of the effect of these features that would make possible the rational design of antioxidants for potential therapeutic use.

## Conclusions

Based on the above experimental and computational findings, several important conclusions can be drawn. Primarily, the

experimental radical scavenging assays firmly established that the 1,3-diarylhydrazones are effective antioxidants. While their potency varies from assay to assay due to the nature of the radical used, they exhibited excellent activities in the ORAC assay which applies the peroxy radical, a well-known, biologically relevant ROS species. Furthermore, DFT studies were performed to provide answers for a series of structural questions regarding the hydrazones, such as the nature of the active species or the potential contribution of the structural

**Fig. 7** Selected radical scavenging activity vs. calculated parameter plots to illustrate the effect of the physicochemical parameters on the antioxidant activity of the hydrazones depicted on Scheme 1



and energetic factors to the antioxidant effect. The calculations as well as NMR and GC-MS studies revealed that while the tautomeric equilibrium may play a role, the potential concentration of the azo-tautomer in equilibrium and hence its contribution to the effect appear to be negligible. After the several molecular characteristics have been calculated and their effect on the experimental activity has been studied, factors such as bond dissociation energy, and ionization potential have emerged as universal contributors to the activity. Other features such as hydrophilicity or lipophilicity (characterized with logP values) appeared to contribute in certain assays but not in all. Features such as HOMO-LUMO energies or the band gap were found to be irrelevant to the antioxidant activity.

**Acknowledgments** The support of this work by the University of Massachusetts Boston is gratefully acknowledged.

## References

- Kelsey NA, Wilkins HM, Linseman DA (2010) *Molecules* 15: 7792–7814
- Valko M, Leibfrtiz D, Moncol J, Cronin MTD, Mazur M, Telser J (2007) *Int J Biochem Cell Biol* 39:44–84
- Brender DA (2012) Free radicals and antioxidant nutrients. In: Murray RK, Bender DA, Botham KM, Kennely PJ, Rodwell VW, Weil PA (eds) *Harper's illustrated biochemistry*. McGraw-Hill Companies, Inc, New York, pp. 543–548
- Pisoschi AM, Pop A (2015) *Eur J Med Chem* 97:55–74
- Horton W, Török M (2017) Small molecule antioxidants. In: Török B, Drasfield T (eds) *Green chemistry: an inclusive approach*. Elsevier (accepted for publication)
- Bors W, Michel C (2002) *Ann N Y Acad Sci* 957:57–69
- Mitra I, Saha A, Roy K (2013) *Can J Chem* 91:428–441
- Khlebnikov AI, Schepetkin IA, Domina NG, Kirpotina LN, Quinn MT (2007) *Bioorg Med Chem* 15:1749–1770
- Rastija V, Medić-Šarić M (2009) *Eur J Med Chem* 44:400–408
- Amić D, Davidović-Amić D, Bešlo D, Rastija V, Lučić B, Trinajstić N (2007) *Curr Med Chem* 14:827–845
- Silva F, Figuiras A, Gallardo E, Nerin C, Dominges FC (2014) *Food Chem* 145:115–125
- Benayahoum A, Amira-Guebailia H, Houache O (2015) *C R Chimie* 18:149–159
- Török B, Sood A, Bag S, Tulsan R, Ghosh S, Borkin D, Kennedy AR, Melanson M, Madden R, Zhou W, LeVine III H, Török M (2013) *Biochemistry* 52:1137–1148
- Zou Y, Chang SKC, Gu Y, Qian SA (2011) *J Agric Food Chem* 59: 2268–2276
- Huang D, Ou B, Hampsch-Woodill M, Flanagan JA, Prior RL (2002) *J Agric Food Chem* 50:4437–4444
- Becke AD (1988) *Phys. Rev. a* 38:3098–3100; Lee C, Yang W, Parr RG (1988) *Phys. Rev B* 37:785–789
- Gaussian 09, Revision E.01, Frisch MJ, Trucks GW, Schlegel HB, Scuseria GE; Robb MA, Cheeseman JR, Scalmani G, Barone V, Mennucci B, Petersson GA, Nakatsuji H, Caricato M, Li X, Hratchian HP, Izmaylov AF, Bloino J, Zheng G, Sonnenberg JL, Hada M, Ehara M, Toyota K, Fukuda R, Hasegawa J, Ishida M, Nakajima T, Honda Y, Kitao O, Nakai H, Vreven T, Montgomery JA Jr., Peralta JE, Ogliaro F, Bearpark M, Heyd JJ, Brothers E, Kudin KN, Staroverov VN, Kobayashi R, Normand J, Raghavachari K, Rendell A, Burant JC, Iyengar SS, Tomasi J, Cossi M, Rega N, Millam JM, Klene M, Knox JE, Cross JB, Bakken V, Adamo C, Jaramillo J, Gomperts R, Stratmann RE, Yazyev O, Austin AJ, Cammi R, Pomelli C, Ochterski JW, Martin RL, Morokuma K, Zakrzewski VG, Voth GA, Salvador P, Dannenberg JJ, Dapprich S, Daniels AD, Farkas Ö, Foresman JB, Ortiz JV, Cioslowski J, Fox DJ (2009) *Gaussian, Inc.*, Wallingford
- Mierts S, Scrocco E, Tomasi J (1981) *Chem Phys* 55:117–129
- Wolinski K, Hilton JF, Pulay P (1990) *J Am Chem Soc* 112:8251–8260
- Rosini M, Simoni E, Milelli A, Minarini A, Melchiorre C (2014) *J Med Chem* 57:2821–2831
- Magalhães LM, Segundo MA, Reis S, Lima JLFC (2008) *Anal Chim Acta* 613:1–19
- Cao G, Alessio HM, Cutler RG (1993) *Free Radic Biol Med* 14: 303–311
- Balsano C, Alisi A (2009) *Curr. Pharm Des* 15:3063–3073
- Ono K, Condrón MM, Ho L, Wang J, Zhao W, Pasinetti GM, Teplow DB (2008) *J Biol Chem* 283:32176–32187
- Berg R, Haenen G, Berg H, Bast A (1999) *Food Chem* 66:511–517
- Apak R, Özyürek M, Güçlü K, Çapanoğlu E (2016) *J Agric Food Chem* 64:1028–1045
- Paiva SA, Russell RM (1999) *J Am Coll Nutr* 18:426–433
- Hegazy WH (2001) *Monatsh Chem* 132:639–650
- Apak R, Özyürek M, Güçlü K, Çapanoğlu E (2016) *J Agric Food Chem* 64:997–927
- Alov P, Tsakova I, Pajeva I (2015) *Curr Top Med Chem* 15:85–104
- Rodriguez SA (2014) Baumgartner MT (2014) *Chem. Phys Lett* 601:116–123
- Kareem HS, Ariffin A, Nordin N, Heidelberg T, Abdul-Aziz A, Wong KW, Yehye WA (2015) *Eur J Med Chem* 103:497–505
- Rouaiguia-Bouakkaz S, Benayahoum A (2015) *J Phys Org Chem* 28:714–722